Rare Metal Materials and Engineering
Volume 50, Issue 12, December 2021
Available online at www.rmme.ac.cn

Science Press

Cite this article as: Yang Lu, Xiong Ji, Guo Zhixing, et al. Microstructure and Properties of Ti(C_x,N_{1-x})-based Cermets with Different C/N Ratios[J]. Rare Metal Materials and Engineering, 2021, 50(12): 4272-4281.

ARTICLE

Microstructure and Properties of Ti(C_x, N_{1-x})-based Cermets with Different C/N Ratios

Yang Lu, Xiong Ji, Guo Zhixing, Liu Junbo, Gou Qingshan, Li Xiangrong

School of Mechanical Engineering, Sichuan University, Chengdu 610065, China

Abstract: Ti(C_x,N_{1-x})-based cermets are fabricated with different ratios of carbon to nitrogen. The effect of C/N ratio on the core-rim structures and properties of cermets was studied. The results indicate that Ti($C_{0.5}$,$N_{0.5}$)-based cermets possess poor properties due to too many pores. With the increase of C/N ratio, the formation rate of white-core/gray-rims decreases, and the homogeneity of the microstructure is enhanced. Consequently, the Ti($C_{0.7}$,$N_{0.3}$)-based cermets show excellent mechanical properties, but a spot of voids and low relative density. TiC-based cermets with excellent relative density and non-porosity can be achieved in the absence of N element, which have coarser grain compared with Ti($C_{0.7}$, $N_{0.3}$) -based cermets. In order to achieve fine grains and high density microstructure, 0.25wt%Cr_3C_2-0.75wt%VC is introduced into the TiC-based cermets. Superior hardness, transverse rupture strength and toughness are achieved. In addition, 0.25wt% Cr_3C_2-0.75wt% VC is also added into the Ti($C_{0.7}$, $N_{0.3}$) -based cermets, but its mechanical properties are lower than that of the Ti($C_{0.7}$,$N_{0.3}$)-based cermets without 0.25wt%Cr_3C_2-0.75wt%VC addition, which is due to acute solid solution reaction of finer and reactive particles with Ti(C,N). The cutting and friction performances of Ti(C_x,N_{1-x})-based cermets with different C/N ratios were also investigated. The results show that the TiC-based cermets with 0.25wt%Cr_3C_2-0.75wt% VC exhibit the lowest coefficient of friction which is 0.15 at the room temperature, and the longest service life during high speed cutting at 1000 r/min.

Key words: core-rim structure; homogeneity; cutting performance; voids

Ti(C_x, N_{1-x}) cermets have drawn wide attention in the past decades owing to their high hardness, chemical inertness, high-temperature stability and excellent wear resistance[1,2]. They are widely used to semi-finishing and finishing steel[3]. In comparison to conventional WC-based tool materials, the microstructures of cermets are more complex[4-6]. Generally, the microstructure of cermets consists of core-rim structure (CRS) including white-core/gray-rim structure and black-core/gray-rim structure. During the solid-state diffusion process, the formation of CRS begins with the aggregation of the inner-rim, and then the outer-rim is formed by the mechanism of dissolution-reprecipitation[7-9].

The formation mechanism of the CRS is conditioned by the presence of a liquid phase during sintering and the original composition of cermets promotes the appearance of this particular microstructure. Liu et al[10] reported that cermets with fine CRS can be fabricated by ultra-fine or nano-powders, which exhibit the excellent transverse rupture strength. Jin[11] and Rajiabi[12] et al concluded that phase transformation of solid solution powders during synthesis refines CRS and improves the toughness of cermets. Furthermore, some researches illustrated that nitrogen element improves the fracture toughness of cermets[13]. And the maximum tool life value is obtained when the ratio of [N]/[N]+[C] is approximately 3 and 5. Peng[14] discovered that TiN prevents the crack propagation, since it promotes a complete rim phase and reinforces the unity between the white-core/gray-rim structure and black-core/gray-rim structure. Although the addition of TiN improves the properties of the cermets, there are some inevitable shortcomings. Compared with TiC powder, the production of Ti(C_{1-x}, N_x) needs to be conducted under nitrogen atmosphere[15]. Meanwhile, the

Received date: December 01, 2020
Foundation item: National Natural Science Foundation of China (51634006, 51901195); Science and Technology Major Project of Sichuan Province (2020ZDZX0022); SCU-Pan Zhi Hua Project (2018CDPZH-25); SCU-Zi Gong Project (2019CDZG-1); National Science and Technology Major Project of China (2019ZX04007001)
Corresponding author: Xiong Ji, Ph. D., Professor, School of Mechanical Engineering, Sichuan University, Chengdu 610065, P. R. China, E-mail: 13668149296@163.com

accurate control of C/N ratio also increases the cost of $Ti(C_{1-x},N_x)$ powder. It is difficult to exactly control the nitrogen content of the cermets. A small number of nitrogen will overflow from $Ti(C_{1-x},N_x)$ during the sintering process, which causes defect (like porosity)[16]. In addition, some researchers indicated that TiN exhibits a poor wettability with binder phase and affects the formation of CRS[17].

Some scholars also found that adding second-phase carbide has an effect on the inner-rim/outer-rim formation of CRS. According to Ref.[18,19], the addition of Mo_2C can promote the generation of CRS, and improve wettability. Moreover, Mo_2C promotes the formation of the inner rim at the outer rim, which effectively prevents atoms from diffusing through liquid phase diffusion. Zhin[20] reported that the black core becomes finer and the grey rim becomes thicker due to the addition of Cr_2C_3/VC, and CRS is remarkably refined with the addition of 0.25wt%Cr3C2-0.75wt%VC. What's more, the addition of NbC, TaC and WC to cermets is also investigated by some scholars, and they have a view that proper carbides can ensure the uniformity and fineness of the CRS[21-23]. Therefore, it is of great importance to obtain excellent CRS without nitrogen. However, the effect of nitrogen on white-core/gray-rim structure and black-core/gray-rim structure of cermets is seldom discussed in previous literatures.

In this work, the influence of different ratios of carbon to nitrogen on the mechanical properties of cermets was studied. Based on this, TiC-based cermets were further refined by adding 0.25wt%Cr3C2-0.75wt%VC. The cutting performance of cermets was also investigated, according to tool life, flank wear and surface processing quality of the workpiece.

1 Experiment

Cermets were prepared through powder metallurgy method, and the composition of cermet samples is shown in Table 1. The raw powder 0.25wt%Cr_3C_2-0.75wt%VC was added into the sample L4 and L5, because the grains were refined most remarkably [20]. Characteristics of raw powders are listed in Table 2. The raw powders were milled in stainless steel jar with cemented carbide balls (10 mm in diameter) at a milling speed of 56 r/min for 72 h. Petrol was added into stainless steel jar as a role mill medium, and the ball-to-powder mass ratio was 10: 1. Then, the slurry powders were dried in a vacuum drying oven. Rubber forming agent was added into dried powders. The powders were sieved through an 80-mesh screen to prevent powder from agglomeration. After that, sieved powders were pressed into rectangular insert blanks with actual dimension of 6.5 mm×5.25 mm×20 mm and triangular insert blanks at a pressure of 250 MPa for the test of basic mechanical properties and cutting performance, respectively. The pressed green pieces were sintered in a vacuum furnace at 1440 °C for 1 h.

The physical properties were measured after the sintered samples were polished. The measured properties include the transverse rupture strength (TRS), Vickers hardness (HV), relative density (RD) and fracture toughness[24]. The scanning electron microscope (SEM) was used to measure the size of grains. The elements of the CRS of the cermets were analyzed by energy dispersive spectrometer (EDS). Grain size of sintered samples was measured by linear intercept method.

The electron probe micro analysis (EPMA) was used to obtain more accurate elemental composition data, especially C

Table 1 Targeted composition of the cermet samples (wt%)

Sample	$Ti(C_{1-x},N_x)$	WC	NbC	Mo_2C	Ni	Co	VC	Cr_3C_2
L1	45 (x=0.5)	27.5	8	1.5	8	10	-	-
L2	45 (x=0.3)	27.5	8	1.5	8	10	-	-
L3	45 (x=0)	27.5	8	1.5	8	10	-	-
L4	45 (x=0)	26.5	8	1.5	8	10	0.75	0.25
L5	45 (x=0.3)	26.5	8	1.5	8	10	0.75	0.25

Table 2 Characteristics of the raw powders

Raw powder	Toltal carbon content/wt%	Free carbon content/wt%	Oxygen content/wt%	Mean particle size/μm
TiC	6.54	0.10	0.20	1.03
$Ti(C_{0.5},N_{0.5})$	8.74	0.06	0.30	1.73
$Ti(C_{0.7},N_{0.3})$	12.87	0.08	0.30	1.85
WC	5.89	0.14	0.30	1.01
NbC	5.72	0.15	0.30	1.32
Mo_2C	6.02	0.20	0.52	1.55
Ni	0.10	0.05	0.10	2.60
Co	0.03	0.05	0.50	1.50
VC	5.81	0.13	0.27	1.10
Cr_2C_3	6.13	0.21	0.18	1.84

and N. X-ray diffraction (XRD) experiments were undertaken on a Philips PW-1700 apparatus using Cu-Kα radiation (λ = 0.154 056 nm). The thermal conductivity was measured by thermal conductivity tester (DRE-2c. Xiangke, China).

The cutting tests were conducted on a CA6140 lathe. The finished cermet insert which is based on Sandvik TNMC06040 8L-GU type blade design is shown in Fig. 1. Cutting parameters include cutting speed (V_c), depth of cutting (A_p) and feed rate (f) are listed in Table 3. The cutting performance of cermets with different CRS was investigated. Meanwhile, the C45 tempered steel was machined under dry cutting condition. The detailed chemical composition of C45 steel is listed in Table 4. Flank wear (VBB) was measured to evaluate the cutting performance of inserts, and VBB was measured at intervals until it was larger than 0.3 mm or the inserts were chipped. Then SEM and EDS facilities were used to analyze the situation of flank wear or chipping.

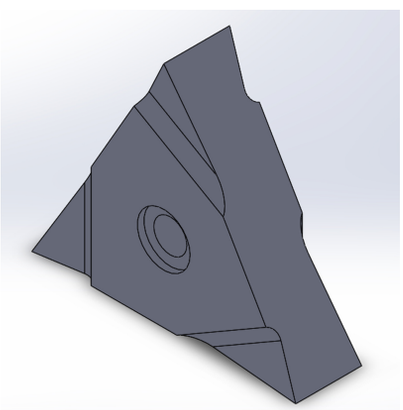

Fig. 1 Shape of the pressed regular triangle blade without groove after grinding

Table 3 Parameters for cutting performance test

Experiment No.	V_c/r·min^{-1}	A_p/mm	f/mm·r^{-1}
1	800	0.1	0.05
2	1000	0.1	0.05
3	800	0.1	0.07
4	800	0.1	0.09

Table 4 Chemical composition of C45 tempered steel (wt%)

C	Si	Mn	Cr	P	S	Ni	Cu
0.42~0.50	0.18	0.58	0.18	0.023	0.016	0.21	0.23

2 Results and Discussion

2.1 Microstructure of cermets

Fig. 2 shows the distribution of white core-rim structure (WCRS) and black core-rim structure (BCRS). Various grains are observed in Fig.2. It is reported that BCRS and WCRS are typical structures of conventional cermets[25]. It is obvious that there are more WCRS and BCRS in L1 and L2 than in L3 and L4 samples, as shown in Fig. 2a~2d. Generally, pure TiC particles possess a higher surface energy than the $TiC_{0.7}N_{0.3}$ and $TiC_{0.5}N_{0.5}$ particles. The second carbides preferentially grow on the undissolved TiC particles during the sintering and form gray rims[26-28]. Thus, for the samples without nitrogen atoms (L3 and L4), there are many grains with thick gray rims. On the contrary, for the samples with nitrogen atoms, the carbides tend to form new cores rather than to grow on the undissolved TiC particles. Therefore, for L1, L2 and L5 samples, plenty of cores with thin rims are obtained. But, obvious voids exist in the microstructure of L1 and L2 samples, and there are more voids in sample L1 than in sample L2. The addition of 0.75wt%VC-0.25wt%Cr_3C_2 causes uneven grain distribution, compared with the sample L2. In

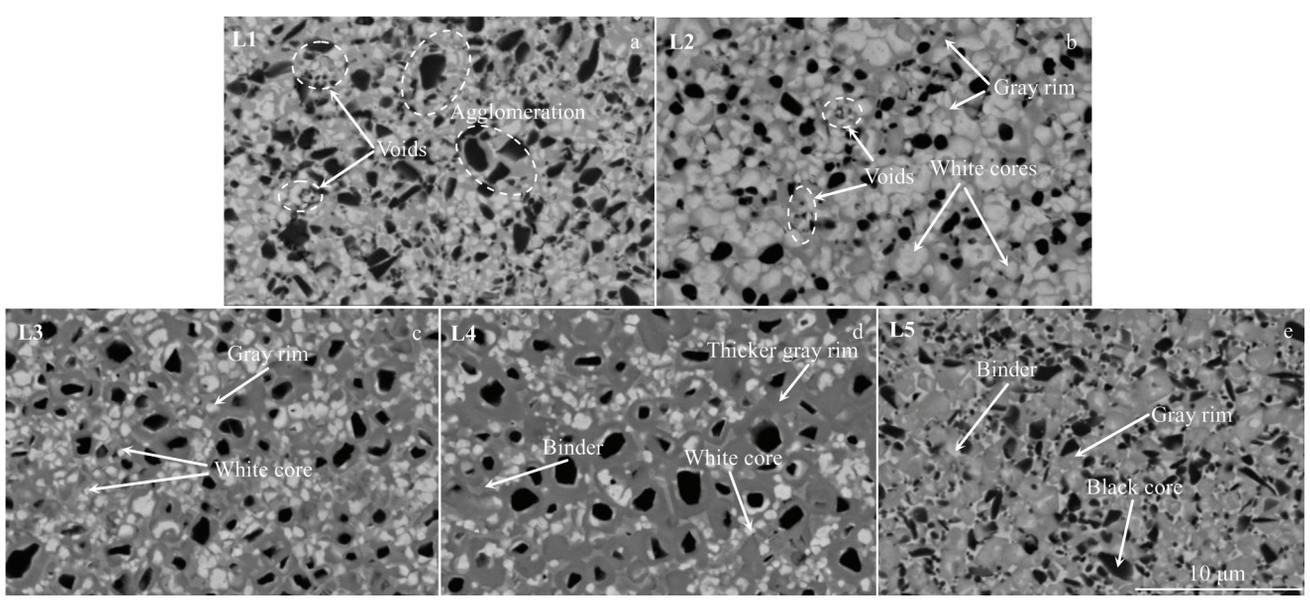

Fig.2 Backscattered electron images of Ti(C_{1-x},N_x)-based cermet samples: (a) L1, (b) L2, (c) L3, (d) L4, and (e) L5

addition, the white core in sample L5 has a tendency to further dissolve into the gray rim.

There is an obvious difference in the grain size of L1~L5 samples in Fig. 3. The mean grain sizes of the five groups of samples are 1.14, 0.92, 1.05 0.98 and 1.01 μm from L1 to L5, respectively. It confirms that TiN hinders the growth of black cores. In addition, the effect is the most obvious when the [N]/[C]+[N] ratio is 30%[12,29]. As a result, the grain size of L2 is finer than that of L1. Meanwhile, the grains size of L1 is larger than that of L3. Because excessive TiN will reduce the wettability[17], and insufficiently wetted particles are easy to aggregate. However, finer CRS can also be obtained by the addition of grain inhibitor. Further comparison between L3 and L4 shows that the CRS of L4 is significantly finer than that of L3, owing to the addition of VC and Cr_3C_2. Generally, most of VC and Cr_3C_2 form segregation at the interface of TiC during liquid phase sintering, preventing the migration of grain boundaries[20]. The inhibitors suppress the growth of TiC grains caused by particle aggregation. Moreover, a small amount of Cr_3C_2 and VC dissolve in the rim phase, which reduces the solubility of Ti and C atoms in the binder phase and decreases the formation rate of black cores[20]. However, the grain size of sample L5 added with 0.75wt%VC-0.25wt% Cr_3C_2 is larger than that of L2 after introduction of N and VC-Cr_3C_2. The refining mechanisms of TiN and VC-Cr_3C_2 are different. On the one hand, TiN mainly inhibits the solid solution reaction of various carbides with $TiC_{1-x}N_x$, and thus the thickness of the rim phase is reduced[30]. From Fig. 2a~2c, it can be seen that the thickness of the rim gradually decreases with increasing the N content. However, a large amount of nitrogen can reduce the wettability between $TiC_{1-x}N_x$ and Ni binder, leading to the aggregation of $TiC_{1-x}N_x$ particles. Therefore, L1 has the biggest mean grain size.

On the other hand, VC-Cr_3C_2 mainly inhibits the grain growth of WC phase or (Ti, W, Nb, Mo)C solid solution phase by adsorption, reducing dissolution rate and lowering grain boundary migration[31]. From Fig. 2c and 2d, it is obvious that the grain size of the white core in L4 is much finer, but the rim becomes thicker. It is deduced that the fine WC phase or WC-base solid solution phase (W, Ti, Nb, Mo) can easily react with $TiC_{1-x}N_x$, resulting in thicker gray rim. Therefore, the grain size of L4 is slightly larger than that of L2. However, the synergistic effect of TiN and VC-Cr_3C_2 cannot result in finer grain size of cermet L5. From Fig. 2e, the white cores even disappear due to acute solid solution reaction of the finer and reactive particles with Ti(C, N). Therefore, L5 with both TiN and VC-Cr_3C_2 shows larger mean grain size than L2 and L4.

The sample L2 was analyzed by EPMA (Fig. 4), and three distinct phases are pointed out: point 1 represents the component at the black core, point 2 represents the component at the white core, and point 3 represents the component in the gray rim. EPMA dot analysis in these areas shows that the C/N ratio in the black core is close to 7:3, and that in the metal binder phase is much larger than it, which may be due to the diffusion of other carbon atoms or the nitrogen atoms lost during sintering. This is the reason why nitrogen-containing cermets have voids.

Fig. 5a shows XRD patterns of the densified cermets after sintering, including ceramic phase and metal phase. Xiao[17] and Yan[19] et al have confirmed that Mo_2C is dissolved during the sintering process and then forms the shell to re-precipitate on black core. The comparison among sample L1, L2 and L3 turns out that the metal binder phase shifts toward lower angles with increasing the nitrogen content, as shown in Fig. 5b. So nitrogen promotes molybdenum carbide to dissolve in the metal phase at the liquid phase sintering stage, and it is

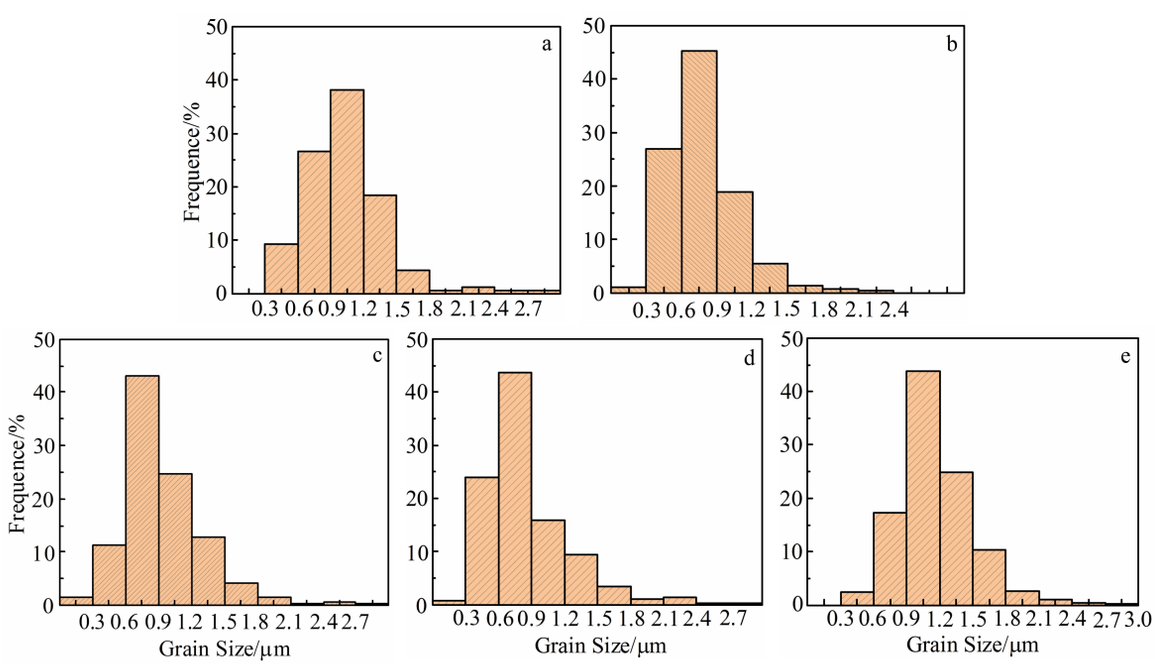

Fig.3 Grain size distribution of different sintered TiC-based cermets samples: (a) L1, (b) L2, (c) L3, (d) L4, and (e) L5

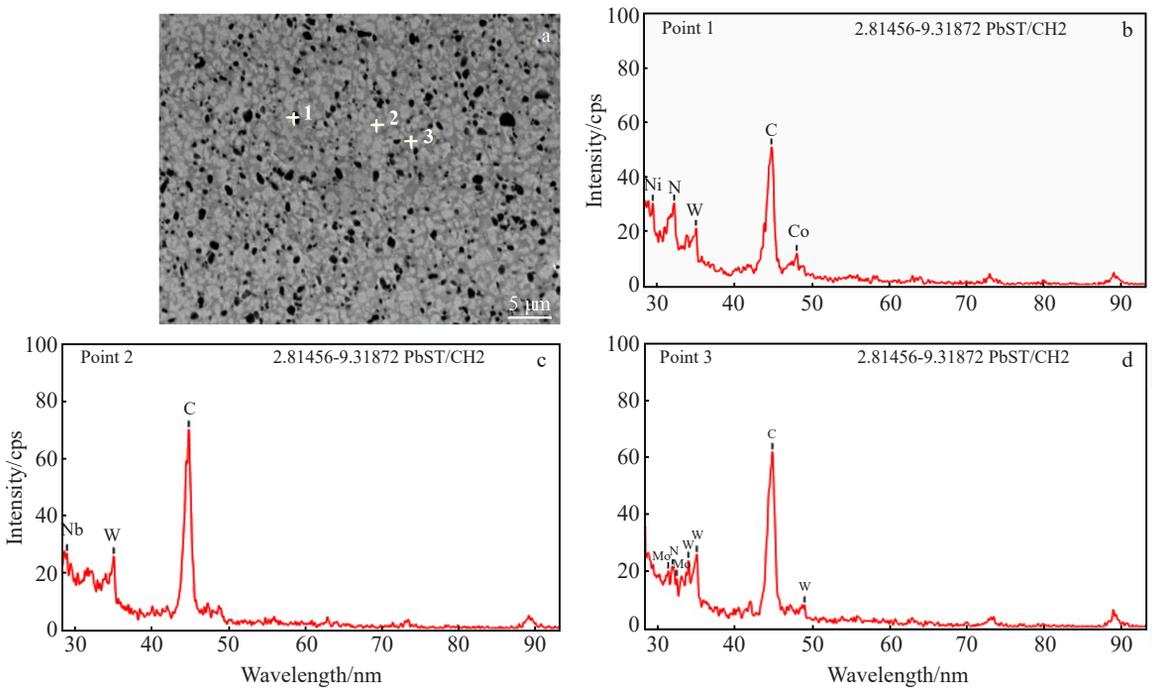

Fig.4 Microstructure of sample L2 (a) and corresponding EPMA analysis results of point 1 (b), point 2 (c) and point 3 (d)

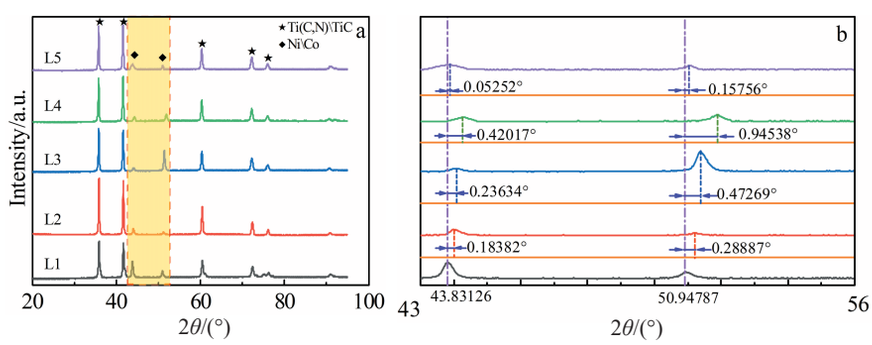

Fig.5 XRD patterns of the densified cermet samples after sintering (a) and magnification in the 43°~56° region (b)

easier to form a Mo_2C shell on TiC or TiCN particles below 1200 °C[32]. Then, the smaller atoms (such as Ti, C, N) cannot gather in the core through the liquid phase, but only dissolve in the liquid phase. It draws a conclusion from above discussions that the binder phase has more solid solutions. The angle of the diffraction peak of sample L3 is low in comparison with that of sample L4, because a small amount of VC and Cr_3C_2 are dissolved in liquid phase, reducing the solubility of Ti and C atoms in liquid. Thereby the metal phase is at a larger angle. The angle of the diffraction peak of sample L5 is low in comparison with that of sample L2. It is possible that more elements are dissolved in the bonding phase of sample L5.

The basic mechanical properties of the cermets, such as the relative density, transverse fracture strength (TRS), Vickers hardness (HV), fracture toughness (K_{IC}) and thermal conductivity of cermets are shown in Table 5. In addition, the relative density of L1 to L5 is about 98.13%, 98.97%,

Table 5 Mechanical properties of cermet samples

Sample	Relative density/%	Hardness, HV_{30}/×10 MPa	TRS/MPa	K_{IC}/MP·m$^{1/2}$	Thermal conductivity/W·(m·K)$^{-1}$
L1	98.13±0.284	1483±40.4	1797±54.6	8.78±0.20	76.54±0.06
L2	98.97±0.153	1593±34.1	2046±36.7	9.33±0.13	76.83±0.03
L3	99.26±0.055	1543±31.5	2113±44.0	8.94±0.19	77.06±0.04
L4	99.12±0.161	1624±23.3	2282±47.1	9.06±0.24	77.00±0.04
L5	98.82±0.147	1561±36.7	1932±50.5	9.12±0.17	76.79±0.06

99.26%, 99.12% and 98.82%, respectively. The relative density gradually increases from L1 to L3 samples, which may be caused by the following two reasons. On the one hand, it is possible that incomplete degumming causes matrix defects (like voids). On the other hand, the relative density of TiN powder is lower than that of TiC powder. It is a reasonable explanation that TiN-containing cermets generate a certain amount of nitrogen overflowing and increase the porosity in the substrate. The Vickers hardness (HV) increases monotonically from 14 830 MPa to 16 240 MPa as CRS changes. The reason why sample L4 has excellent hardness is because the inherent hardness of TiN is lower than that of TiC, and the finer CRS is another reason. The TRS increases to 2113 MPa, from L1 to L3. It is implied that the sample L3 has a better transverse fracture strength. Three reasons are illustrated as follows. Firstly, the substrate has some defects caused by pores. Secondly, it is possible that the wettability of TiN to the liquid phase is lower than that of TiC to metals[17]. The last reason can be obtained from Fig. 5b, which exhibits the diffraction peaks of the liquid phases shifting to the higher angle direction from L1 to L4. The mechanical properties of the sample L5 are lower than that of the sample L2. It shows that TiN and 0.75wt% VC-0.25wt% Cr_3C_2 cannot improve the properties of the cermets, due to acute solid solution reaction of the finer and reactive particles with Ti(C,N). The toughness of cermets without TiN addition is lower than that of the sample groups with TiN addition, which also demonstrates the results of Ref. [10]. In the above case, adding VC and Cr_3C_2 can further make the grains finer, thereby obtaining sample L4, according to the Hall-Petch relation[20]. Although these samples have minor differences in composition, the difference of relative density determines the difference in thermal conductivity. As shown in Table 5, the thermal conductivity of the sample with higher relative density is also higher.

2.2 Cutting performance

2.2.1 Tool life

The tool life is affected by many factors, such as the material of workpiece, cutting fluid, and cutting parameters. Moreover, the wear resistance is the most significant factor affecting inserts life. The flank wear (VBB) is considered to be the main cause of destruction during turning[32]. So, the service life of inserts is always evaluated by flank wear. After the VBB value reaches a certain limit, it will have a certain negative effect on the machining accuracy, workpiece surface quality and processing efficiency. Thus, the value of VBB is directly used to evaluate the properties of cutting tools. When the flank wear value reaches 0.3 mm, the insert enters the failure stage (ISO standard 3685). Three independent variables can be observed from the experiment: depth of cut (A_p), feed rate (f), and cutting speed (V_c). In this experiment, the A_p was ignored since the inherent groove shape of the inserts cannot be adapted to a large depth of cutting. In other words, the undischarged chips continue to rotate on the workpiece, breaking the tools surface. In Fig. 6 and Fig. 7, flank wear is measured with increasing the cutting speed (V_c) and feed rate (f), respectively. Positive effect is shown on 0.25wt%-0.75wt% Cr_3C_2-TiC cermets (L4). The service life of sample L4 is the longest. This phenomenon may be concerned

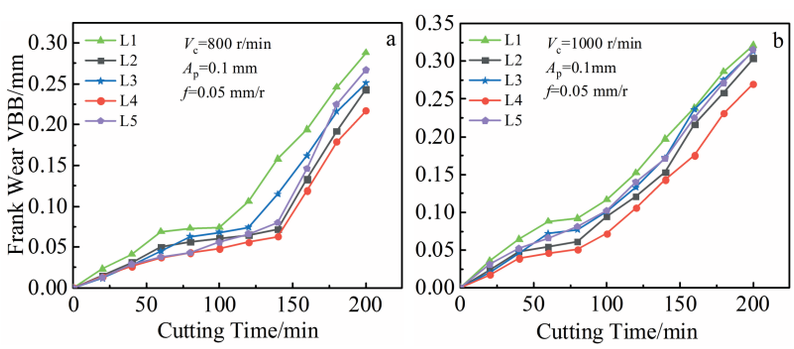

Fig.6 Flank wear VBB values of different cermet samples with cutting speeds of 800 r/min (a) and 1000 r/min (b)

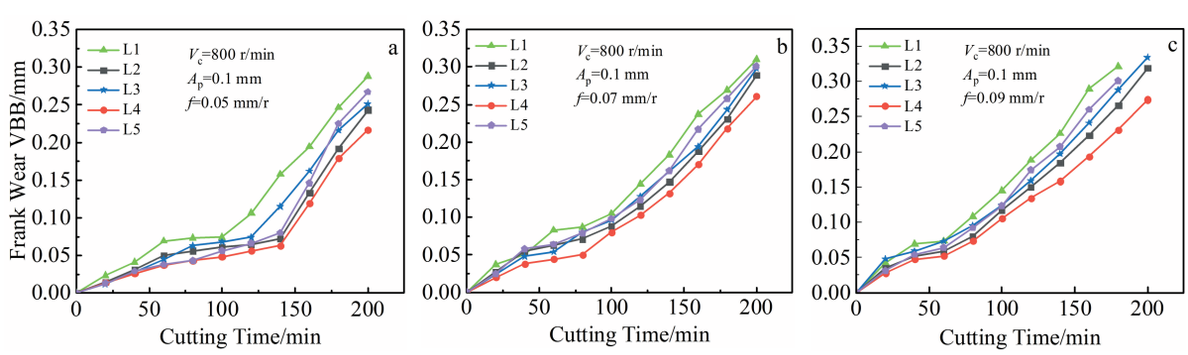

Fig.7 Flank wear VBB values of different cermet samples with different feed rates: (a) 0.05 mm/r, (b) 0.07 mm/r, and (c) 0.09 mm/r

with the excellent mechanical properties or energy absorption of non-ceramic bonding phase[33]. The tool life of the experimental group L1 is the shortest, which may be the result of the combined effect of the mechanical properties and internal defects.

The wear stage of the tool can be divided into three stages from Fig.6 and Fig.7: running-in wear is the initial stage with a small amount of wear, then stable wear expresses slow wear, and finally severe wear implies that the tool is about to fail. Therefore, in Fig.6a, increasing the cutting speed can directly induce higher temperature in the contact area, which is a key factor affecting the tool of stable wear stage. High temperature may result in more serious thermal stress and thus reduce the mechanical properties of the tool. Furthermore, when the cutting speed is 800 r/min, the stable wear stage appears earlier in comparison with that at cutting speed of 1000 r/min. Comparing the sample L2 with sample L3, it can be noted that the flank wear rate of the samples L2 and L3 is roughly the same at the cutting speed of 800 r/min. L2 has a better cutting performance under the cutting conditions of 1000 r/min, because L2 has better fracture toughness than L3, according to Table 5. As the overall mechanical performance of L5 is lower than that of L2, the service life of sample L2 is higher than that of sample L5.

As discussed above, the 0.25wt% VC-0.75wt% Cr_3C_2-TiC-cermets show the longest life among all inserts at different cutting speeds. In addition, sample L2 has a better cutting performance than sample L3. It indicates that the insert L4 is more suitable than insert L3 under high speed with the same feed rate as well as depth. In order to further discuss the effect of feed rate on the cermets, the depth and the cutting speed of inserts are selected at 0.1 mm and 800 r/min, respectively. Then the feed rate is set at 0.05, 0.07 and 0.09 mm/r. The detailed results are shown in Fig.7. As the feed rate increases, the stable wear stage of the tool is shortened. Simultaneously, L4 and L2 have excellent service life, especially the sample L4 has the longest service life.

2.2.2 Wear mechanism

Friction and extrusion on the contact surface between workpieces and inserts will cause wear and damage on the tools surface. The morphologies of flank wear, at the feed rate of 0.05 mm/r, cutting depth of 0.1 mm and speed of 1000 r/min, are shown in Fig.8. From Fig.8, the failure mechanism of the cermets is mainly due to abrasive wear, adhesive wear and diffusion wear. The inserts of L1, L3 and L5 have fractures on the tool edges. L1 is worn badly. For all the groups of cermets, bumpy textures can be found which parallels to the feed direction. Although the damage degrees of the insert L2 and insert L4 are almost the same, the wear mechanism is different. The adhesive wear mainly occurs on the L2. However, more fine grooves are found in the sample L4. It indicates that abrasive wear plays a significant role in L4. There are obvious phenomena that the wear mechanisms mentioned above exist on every inserts body. And these three types of wear mechanisms generally co-exist[34]. During the cutting procedure, atom diffusion and inserts oxidation occur due to the local high temperature. Fig.9 depicts that lots of Fe and O atoms are attached to the surface of each sample. On the one hand, the atoms of the same main group (such as Fe, Co, and Ni) undergo atomic diffusion under a high-temperature friction conditions, leading to adhesive wear and the absence of bonding phase framework. On the other hand, the oxidation resistance of samples with the addition of TiN is weaker than that of TiN-free-cermets[35], and the oxygen content of L4 is the least among all the samples, due to the addition Cr_3C_2 and VC. The same phenomenon is also

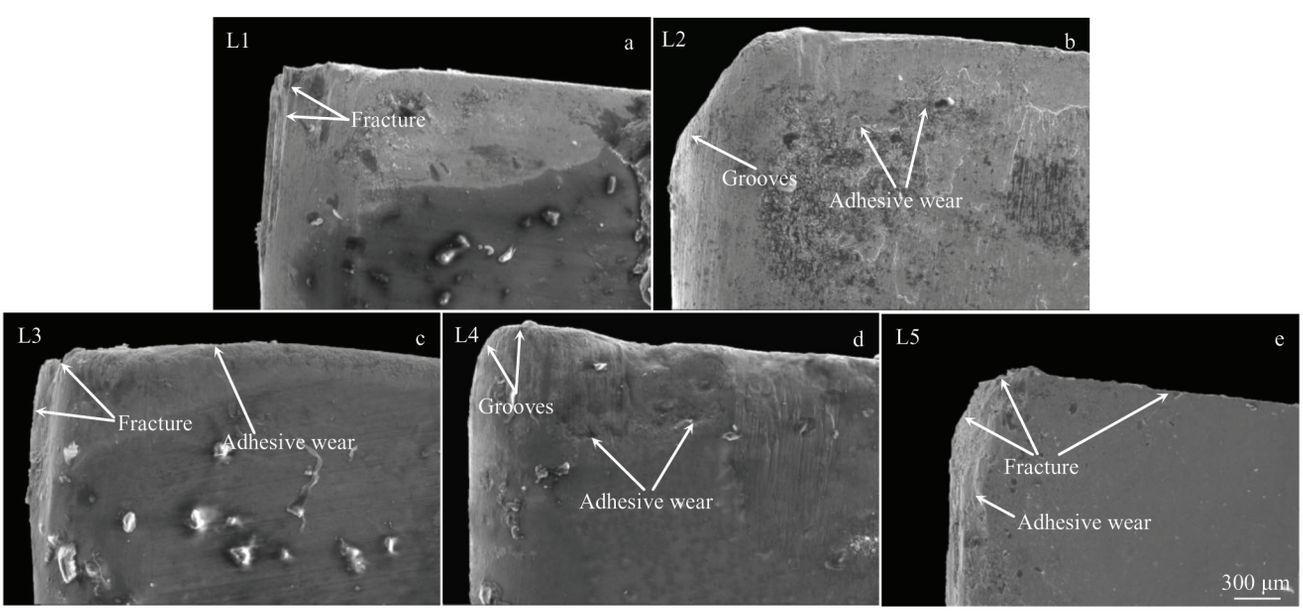

Fig.8 Flank wear morphologies of different cermet inserts after turning C45 steel at cutting speed of 1000 r/min: (a) L1, (b) L2, (c) L3, (d) L4, and (e) L5

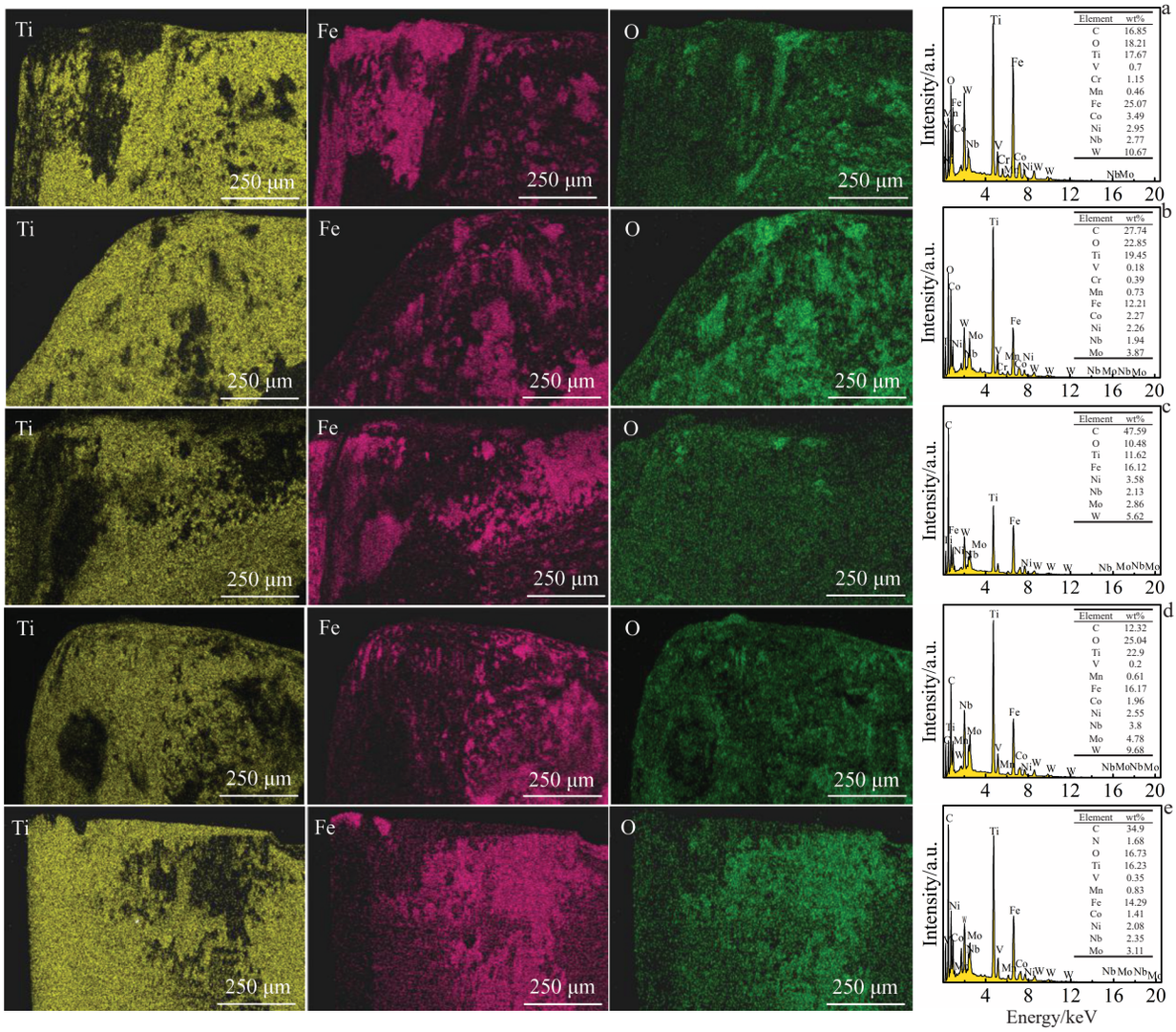

Fig.9 EDS spectra and element mappings of different cermet samples: (a) L1, (b) L2, (c) L3, (d) L4, and (e) L5

founded in sample L5. During the cutting process, the sample L5 shows a slight breaking edge, which is caused by the low transverse breaking strength. Furthermore, abrasive particles originate from the relative motion between tool flank and workpiece. Tool surface is destroyed by ploughing, micro-cutting, and scoring with the abrasive particles. For the sample L4, excellent high-temperature chemical stability, thermal conductivity and mechanical properties contribute to superior wear resistance and anti-oxidation, but diffusion and adhesion are slightly inferior.

2.2.3 Workpiece surface roughness

Fig. 10 shows the coefficient of friction of polished cermet samples at room temperature. There is an inseparable relationship between the coefficient of friction and hardness, and the harder cermets may exhibit a better coefficient of friction before severe wear[36]. Sample L4 has a lower coefficient of friction. Fig. 11 proves that the coefficient of friction has a great influence on the surface roughness (R_a) of the workpiece with the same cutting parameters. The

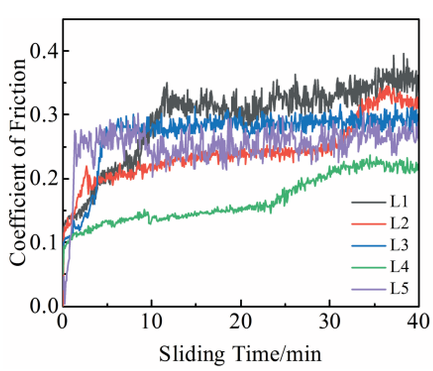

Fig.10 Coefficient of friction of polished cermet samples at room temperature

coefficient of friction is directly related to the cutting force. During the cutting process, the lower coefficient of friction can prolong the service life of the insert and keep the original

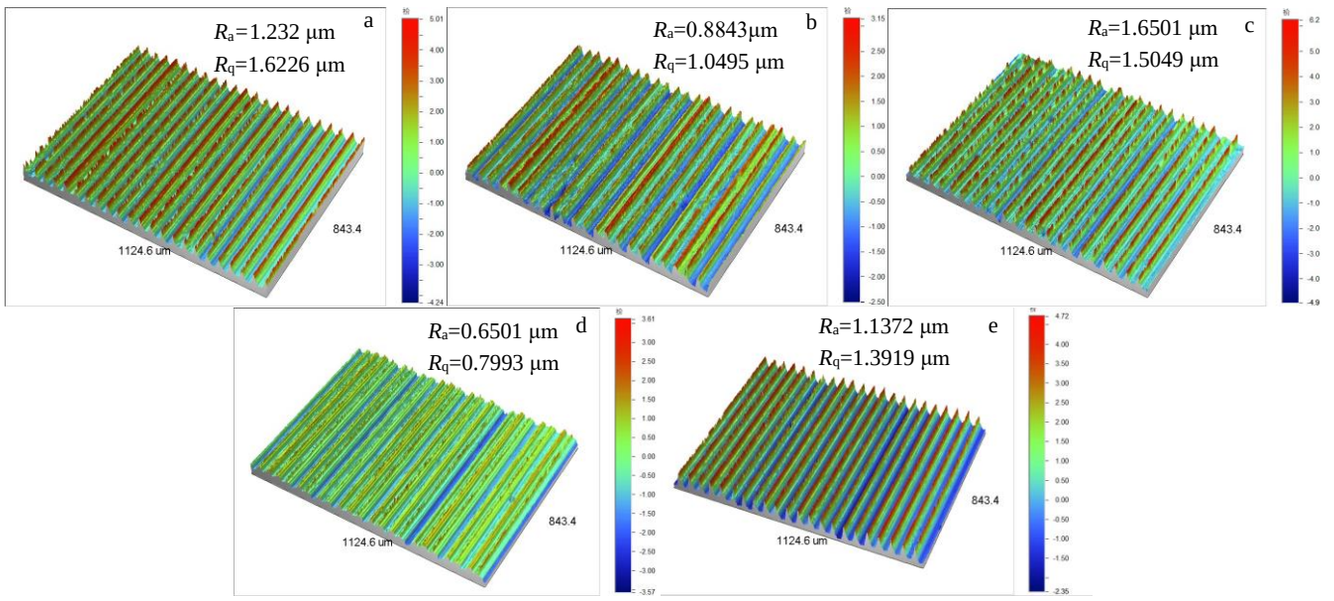

Fig.11 Surface quality of different workpieces after cutting 45 steel for 60 min under the cutting parameters of cutting speed 1000 r/min, feed rate 0.05 mm/r and cutting amount 0.1 mm: (a) L1, (b) L2, (c) L3, (d) L4, and (e) L5

shape of the inserts[37]. Thus, sample L4 can still obtain a good surface roughness on the surface of the workpiece, after processing for a long time.

3 Conclusions

1) In comparison of the five kinds of samples, the Ti($C_{0.5}$,$N_{0.5}$) based cermets have lots of voids and many coarse grains. Although the microstructure of Ti($C_{0.7}$,$N_{0.3}$)-based cermets is finer than that of the TiC-based cermets, the density is lower. The addition 0.75wt% VC-0.25wt% Cr_3C_2 of TiC-based cermets contributes to obtain fine grains without voids. In addition, 0.25wt% Cr_3C_2-0.75wt% VC is also added into the Ti($C_{0.7}$,$N_{0.3}$)-based cermets, but the synergistic effect of TiN and VC-Cr_3C_2 cannot result in finer grain size of cermet due to acute solid solution reaction of the finer and reactive particles with Ti($C_{0.7}$,$N_{0.3}$)-based cermets.

2) TiC based cermets possess better properties and higher density by adding 0.75wt% VC-0.25wt% Cr_2C_3. Additionally, TiC is more stable than TiN. During sintering, the phase transformation of TiC will avoid the defects caused by nitrogen decomposition. TiC-based cermets have thicker rim, due to the diffusion of heavy elements from metal phases to the black core and gray rim. The re-precipitation of heavy elements in Ni/Co binder phase also promotes the increase of the outer rim thickness. The formation rate of white-core/gray-rims decreases and the homogeneity of the microstructure is enhanced, which increases with the ratio of carbon to nitrogen increasing. As the nitrogen content decreases, the dissolution of carbides in the metal phase decreases.

3) When the cutting parameters (cutting speed and feed speed) are changed, the flank wear is recomputed. TiC-based cermets added with 0.75wt% VC-0.25wt% Cr_2C_3 possess the best mechanical property and the longest service life. The wear mechanisms during the cutting process are mainly adhesive wear, abrasive wear and diffusion wear. The increase of the cutting speed and the feed rate can shorten the stable period of flank wear and reduce the life of inserts. The CRS of cermets has a certain effect on the surface roughness of the workpiece. Among the five groups, the coefficient of friction of sample L4 is the smallest, about 0.15, but it is unstable. The lower coefficient of friction of sample L4 contributes to a better surface roughness of workpiece after cutting C45 steel for 60 min. What's more, the ability of 0.75wt% VC-0.25wt% Cr_2C_3-TiC-based cermets to resist deformation is higher than that of other controls.

References

1 Li Jia, Sheng Guangmin. *Rare Metal Mat Eng*[J], 2017, 46(4): 882

2 Ding Kunying, Guo Yafei, Zou Hui. *Rare Metal Mat Eng*[J], 2017, 46(2): 307

3 Wang Haibo, Wang Dongpo, Cheng Fangjie *et al*. *Rare Metal Mat Eng*[J], 2015, 44(12): 2987

4 Cordoba J M, Chicardi E, Francisco J G *et al*. *Journal of Alloys and Compounds*[J], 2013, 559: 34

5 Prasanta Sahoo, Davim J P *et al*. *Tribology for Scientists and Engineers*[M], 2013, 7: 211

6 Ovcharenko V E, Psaknye S G, Ivanov Yu F *et al*. *Rare Metal Mat Eng* [J], 2015, 44(1): 1

7 Wang Jie, Liu Ying, Ye Jinwen. *Rare Metal Mat Eng*[J], 2018, 47(5): 1385

8 Kruse O, Janson S, Frisk K *et al*. *Journal of Phase Equilibria and Diffusion*[J], 2001, 22(5): 552

9 Vinid K. Sarin (Ed), *Comprehensive Hard Materials*[M].

Boston: ELSEVIER
10 Liu Ning, Yin Weihai, Zhu Longwei *et al*. *Mater Sci Eng A*[J] 2007, 445-446: 707
11 Jin Yongzhong, Liu Ying, Wang Yankun *et al*. *Mater Chem Phys* [J], 2009, 118: 191
12 Rajabi A, Ghazali M J, Kevin J *et al*. *Materials and Design*[J], 2015, 67: 95
13 Shi Zengmin, Zhang Dayong, Li Guojun *et al*. *J Alloy Compd*[J], 2013, 568: 68
14 Ying Peng, Miao Hezhou, Peng Zhijian *et al*. *Int J Refract Met Hard Mater*[J], 2013, 39: 78
15 Wei Sen, Xu Baoqiang, Liu Jiantao *et al*. *Trans Nonferrous Met Soc China*[J], 2011, 21: 185
16 Liang Mengxia, Xiong Ji, Guo Zhixing *et al*. *Int J Refract Met Hard Mater*[J], 2014, 43: 322
17 Xiao P, Derby B. *Acta Mater*[J], 1996, 44: 307
18 Guo Zhixing, Xiong Ji, Mei Yang *et al*. *Int J Refract Met Hard Mater*[J], 2008, 26: 601
19 Yan Li, Ning Liu, Rong Chunlan *et al*. *J Refract Met Hard Mater* [J], 2008, 26: 190
20 Zhin Bin, Liu Ning, Jin Zhibo *et al*. *Trans Nonferrous Met*[J], 2012, 22: 1096
21 Kim B K, Ha G H, Marry J K *et al*. *Nanostruct Mater*[J], 1997, 18: 233
22 Lee H R, Kim D J, Jak D C *et al*. *J Am Ceram Soc*[J], 2003, 86: 152
23 Huang S G, Liu R L, Li L *et al*. *Int J Refract Met Hard Mater*[J], 2008, 26: 389
24 You Qianbing , Xiong Ji, Liu Junbo *et al*. *Int J Refract Met Hard Mater*[J], 2019, 81: 299
25 Li Pingping, Ye Jinwen, Liu Ying *et al*. *Int J Refract Met Hard Mater*[J], 2012, 35: 27
26 Ettmayer P, Kolaska H, Lengauer W *et al*. *Int J Refract Met Hard Mater*[J], 1995, 13: 343
27 Xiong J, Guo Z, Chen F J *et al*. *Int J Refract Met Hard Mater*[J], 2007, 25: 367
28 Liu N, Zeng Q, Yang Y *et al*. *Mater Sci Technol*[J], 2001, 17: 1050
29 Sheng Chao, Liu Ning, Yuan Yupeng *et al*. *Ceram In*[J], 2005, 31: 851
30 Moskowitz D, Terner L L. *Mater Sci Eng A*[J],1988, 105: 265
31 Chen Hao, Yang Qiumin, Yang Jiangao *et al*. *J Alloy Compd*[J], 2017, 714: 245
32 Rajabi A, Ghazali M J, Syarif J *et al*. *Chem Eng J*[J], 2014, 255: 445
33 Du Hao, Xiong Ji, Zhao Haibo *et al*. *Appl Surf Sci*[J], 2014, 292: 688
34 Dong Guangneng, Zhang Junfeng, Zhang Dongya *et al*. *Rare Metal Mat Eng*[J], 2011, 40(8): 1334
35 Yue Rengli, Xia Meirong, Wang Meiqiu *et al*. *Appl Surf Sci*[J], 2019, 495: 143 620
36 Podgursky V, Nisumaa R, Adoberg E *et al*. *Wear*[J], 2010, 268: 751
37 Santosh, Mohammed R A, Lokesha M *et al*. *Materials Today*[J], 2020, 24: 1190

不同碳/氮比的 $Ti(C_x, N_{1-x})$基金属陶瓷的显微组织与性能

杨　露，熊　计，郭智兴，刘俊波，苟青山，李相荣
(四川大学 机械工程学院，四川 成都 610065)

摘　要：$Ti(C_x,N_{1-x})$基金属陶瓷是用不同碳氮比制造的。研究了碳/氮比对芯-环结构和金属陶瓷性能的影响。结果表明，由于孔太多，$Ti(C_{0.5},N_{0.5})$基金属陶瓷的性能较差。随着碳/氮比的增加，白核/灰环的形成率降低，并且微观结构的均匀性增强。因此，基于$Ti(C_{0.7},N_{0.3})$的金属陶瓷显示出优异的力学性能，但有少量的孔隙和较低的相对密度。与$Ti(C_{0.7},N_{0.3})$基金属陶瓷相比，TiC基金属陶瓷在没有N元素的情况下具有较高的相对密度且无孔隙，但其晶粒较粗大。为了获得细晶粒和高密度的显微组织，将0.25%Cr_3C_2-0.75%VC（质量分数）引入到TiC基金属陶瓷中，获得了优异的硬度、横向断裂强度和韧性。另外，在$Ti(C_{0.7},N_{0.3})$基金属陶瓷中也添加了0.25%Cr_3C_2-0.75%VC，但其力学性能低于$Ti(C_{0.7},N_{0.3})$的金属陶瓷，这是因为细颗粒和反应颗粒与Ti(C,N)发生了急性固溶反应。研究了基于不同C/N比的$Ti(C_x,N_{1-x})$基金属陶瓷的切削性能和摩擦性能。结果表明，具有0.25%Cr_2C_3-0.75%VC的TiC基金属陶瓷在室温下的摩擦系数最低，为0.15，在1000 r/min的高速切削过程中，使用寿命最长。

关键词：芯-环结构；均匀性；切削性能；孔隙

作者简介：杨　露，男，1995年生，硕士生，四川大学机械工程学院，四川 成都 610065，E-mail：yangluxn163@163.com